Earthquake Engineering, Tenth World Conference © 1992 Balkema, Rotterdam. ISBN 90 5410 060 5

Torsional tests on large in-situ soil columns

Akira Tateishi & Takehira Takayanagi
Taisei Corporation, Tokyo, Japan

Kenji Ishihara
University of Tokyo, Japan

Masao Hayashi
Tokai University, Kanagawa, Japan

Setsuo Iizuka
Nuclear Power Engineering Center, Tokyo, Japan

Sadao Suzuki
Shimizu Corporation, Tokyo, Japan

ABSTRACT: Large-scale field tests were performed by applying cyclic torsional moments to soil columns cut out in a gravel layer to obtain some convincing data needed to establish a methodology for the seismic design of nuclear power plants built on Quaternary deposits. The cyclic deformation characteristics of the in-situ gravel layer subjected to shear strains in a small to large range were investigated. Furthermore, it was verified that existing analytical methods were applicable to simulation analyses of gravel layers.

1 INTRODUCTION

The basic policy in Japan requires nuclear reactor buildings to be built on rock. However, in order to increase available locations for nuclear power plants in future, the investigation of siting technology on Quaternary deposits has been carried out as a project of the Nuclear Power Engineering Center (NUPEC). The large-scale field tests were performed to establish the methodology for the seismic design of nuclear power plants built on Quaternary deposits. This paper describes the results of the dynamic and static torsional tests on large-scale soil columns prepared in-situ and the simulation analyses. Other aspects of this project are described in the companion papers submitted to this Conference. The outline of the project and preliminary test results is described in the paper by Watabe et al. (1991).

2 TEST METHODS

2.1 In-situ soil columns

The test site was selected within the field of the Tadotsu Engineering Laboratory of NUPEC, in Kagawa Prefecture, Japan. The test site was composed of a reclaimed soil 11m thick underlain by a diluvial gravel layer at depths of 11m to 20m which was the test soil of interest. The diluvial gravel layer had the shear wave velocity of 380m/sec and a SPT N-value of 40-50. In order to expose the diluvial gravel layer, the reclaimed soil was excavated, and from this exposed surface two soil columns were cut out by digging annular-shaped trenches of 10m in inner diameter, 80cm wide, and 9m and 5m deep respectively in the gravel layer. The side-face of the trench wall was protected by placing mudwater mortar, and rubber bags were lowered into the annular-shaped trench and inflated with water in order to support the inside soil columns laterally as shown in Fig. 1. Then, capping concrete blocks were mounted on top of the soil columns in order to facilitate transfer of cyclic load from loading devices. The confining pressure existent prior to excavation was applied to the soil columns by the weight of the capping concrete blocks and the water pressure in the rubber bag. The outline of the soil columns is shown in Fig. 1. and Fig. 2.

2.2 Loading method

The dynamic torsional tests were conducted by applying sinusoidal torsional moments to the 9m and 5m deep soil columns by means of two exciters mounted on top of the capping block operating in opposite phase, as shown in Fig. 1. For the 9m deep soil column, the loading moment was increased in 3 steps, 49, 98 and 147kN.m, in order to achieve a small level of shear strain of 10^{-5}. For the 5m deep soil column, the loading moment was increased in 5 steps, 98, 196, 294, 392 and 490kN.m, in order to achieve a medium level of shear strain of 10^{-4}. The loading moment amplitude was constant in each loading step, in which the frequency was changed by an increment of 0.1 Hz.

The static torsional tests were conducted by applying cyclic torsional moments to the 9m deep soil column by means of two hydraulic jacks installed between the capping block and the reaction block operating in opposite phase, as shown in Fig. 2. The loading moment was increased in 6 steps, 8.8, 11.8, 17.7, 23.5, 29.4 and 35.3MN.m, in order to achieve a large

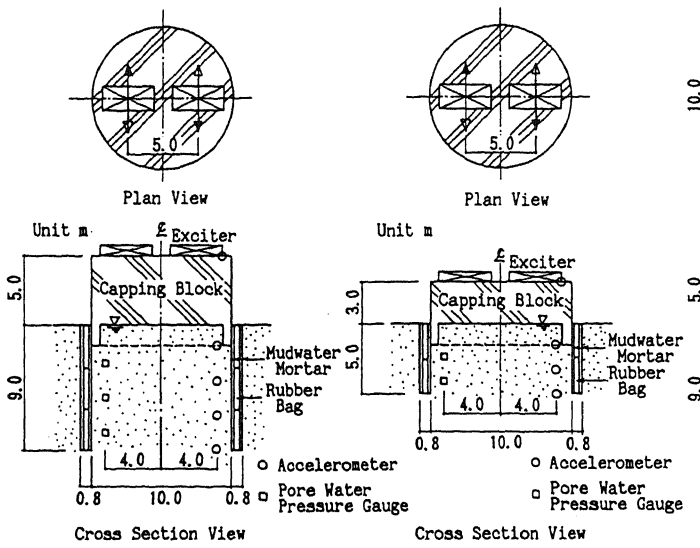

(a) 9m deep soil column (b) 5m deep soil column

Fig. 1 In-situ soil columns for dynamic torsional test

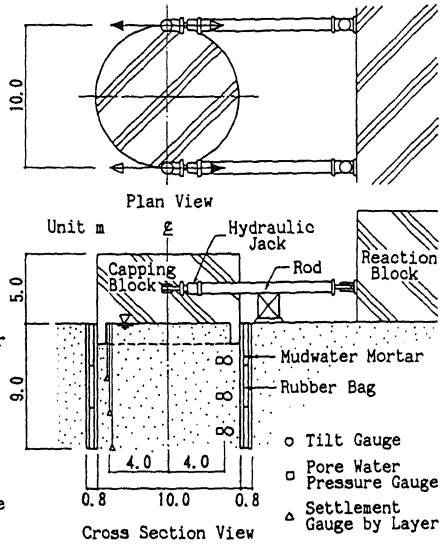

Fig. 2 In-situ soil column for static torsional test

level of shear strain of 10^{-3}. The loading moment amplitude was constant in each loading step, in which 5 cycles of static load with a triangular waveform were applied slowly.

2.3 Measuring instrumentation

In the dynamic torsional tests, the measuring instruments used were accelerometers and pore water pressure gauges, as shown in Fig. 1. The accelerometers were installed to measure tangential accelerations of the capping blocks and the soil columns. The pore water pressure gauges were installed to measure the fluctuation of excess pore water pressures in the soil columns.

In the static torsional tests, the measuring instruments used were tilt gauges, pore water pressure gauges and settlement gauges, as shown in Fig. 2. The tilt gauges were installed to measure tangential shear strains of the soil column. The pore water pressure gauges were installed to measure the fluctuation of excess pore water pressures in the soil column. The settlement gauges were installed to measure the compressive deformations of the soil column in vertical direction.

3 TEST RESULTS

3.1 Dynamic torsional tests

Fig. 3 shows the acceleration resonance curves of the soil columns and Fig. 4 shows the relationships between the shear strain of the soil column at the resonance frequency and the loading moment. The shear strain was calculated thus that the relative displacement was obtained by integrating the acceleration twice and it was divided by the vertical distance between the accelerometers. As shown in Fig. 4, the intended levels of shear strain are achieved for both the 9m and 5m deep soil columns. As shown in Fig. 3, the resonance frequency and the amplification ratio of the acceleration of the 9m deep soil column decrease slightly as the loading moment increases, and those of the 5m deep soil column decrease even more in comparison with the results of the 9m deep soil column. It indicates that the stiffness of the soil columns was reduced and the damping increased as the shear strain increased in the soil columns.

Regarding the pore water pressure, for the 9m deep soil column the excess pore water pressure fluctuated at the same frequency as the loading moment, and for the 5m deep soil column the excess pore water pressure fluctuated at twice the frequency of the loading moment due to the effect of dilatancy. However, for both the 9m and 5m deep soil columns accumulation of the excess pore water pressure was not observed in the shear strain range smaller than 10^{-4}.

3.2 Static torsional tests

Fig. 5 shows the shear strain-loading moment curve of the soil column and Fig. 6 shows the relationships between the shear strain of the soil column and the loading moment at the final cycle. In Fig. 6, one half of a double amplitude of the shear strain at the final cycle is indicated. As shown in Fig. 5, the intended level of shear strain of 10^{-3} is

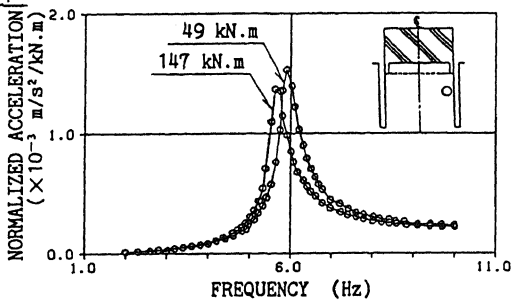

(a) 9m deep soil column

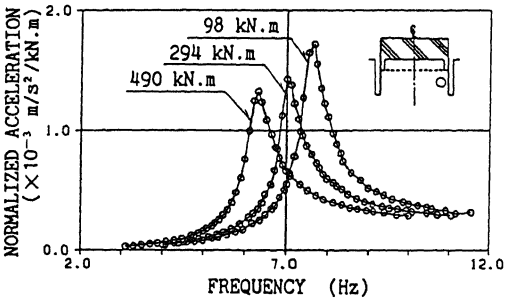

(b) 5m deep soil column

Fig. 3 Acceleration resonance curves in dynamic torsional test

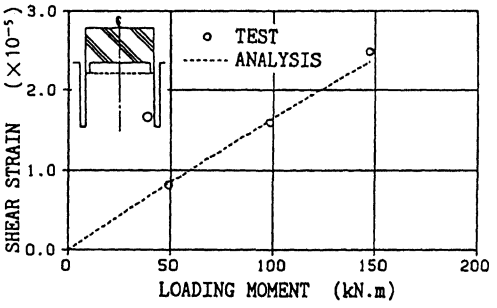

(a) 9m deep soil column

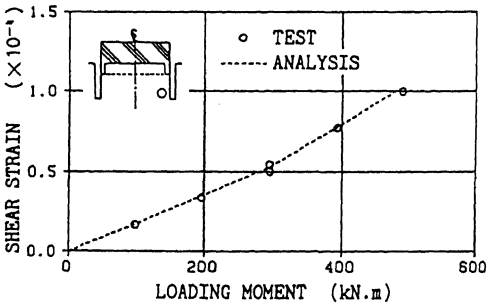

(b) 5m deep soil column

Fig. 4 Relations between shear strain at resonance frequency and loading moment in dynamic torsional test

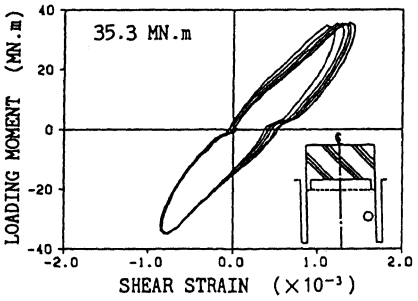

Fig. 5 Shear srain-loading moment curve in static torsional test

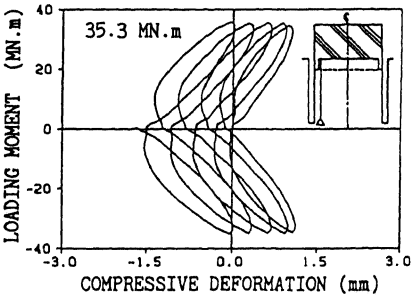

Fig. 7 Compressive deformation-loading moment curve in static torsional test

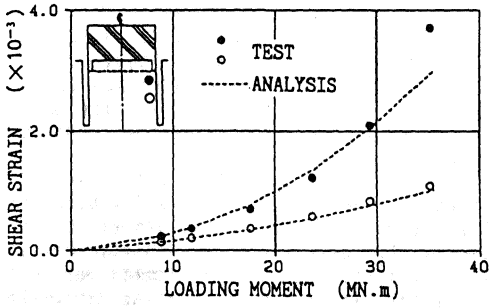

Fig. 6 Relations between shear strain and loading moment in static torsional test

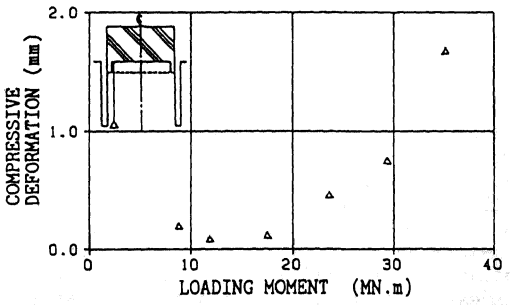

Fig. 8 Relations between residual compressive deformation and loading moment in static torsional test

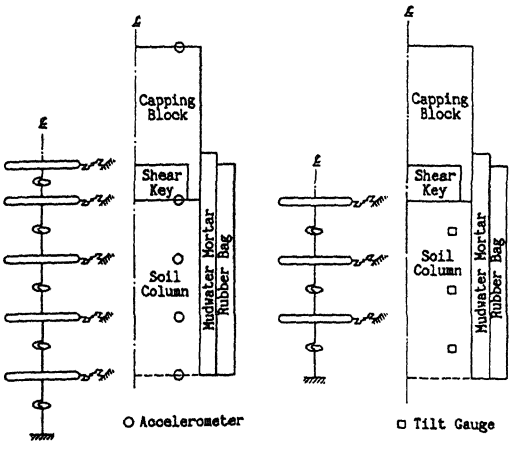

(a) dynamic test (b) static test

Fig. 9 Models of inverse analysis

achieved in the tests. The shear strain-loading moment curve shows a spindle shaped pattern inherent in soil material and it also draws stable hysteresis loops in the large level of shear strain of 10^{-3}. As shown in Fig. 6, the amplification ratio of the shear strain of the soil column increases largely as the loading moment increases. It indicates that the stiffness of the soil column was reduced significantly as the shear strain increased to the level of 10^{-3}.

Regarding the pore water pressure, the excess pore water pressure fluctuated at twice the frequency of the loading moment due to the effect of dilatancy. However, the excess pore water pressure did not accumulate, because halts of operation of the hydraulic jacks for a while at zero loading caused dissipation of the excess pore water pressure. Instead, accumulation of the compressive deformation was observed.

Fig. 7 shows the compressive deformation-loading moment curve in the maximum loading step and Fig. 8 shows the relationships between the residual compressive deformation of the soil column and the loading moment. As shown in Fig. 7, the compressive deformation changes in the direction of extension during loading and changes in the direction of compression during unloading due to the dilatancy inherent in dense sand or gravel material. Then, with increasing number of loading cycle the compressive deformation continues to accumulate in the direction of compression. As shown in Fig. 8, when the loading moment becomes larger than 23.5MN.m the residual compressive deformation increases largely, and accumulation of the residual compressive deformation became noticeable in the shear strain range larger than 10^{-3}.

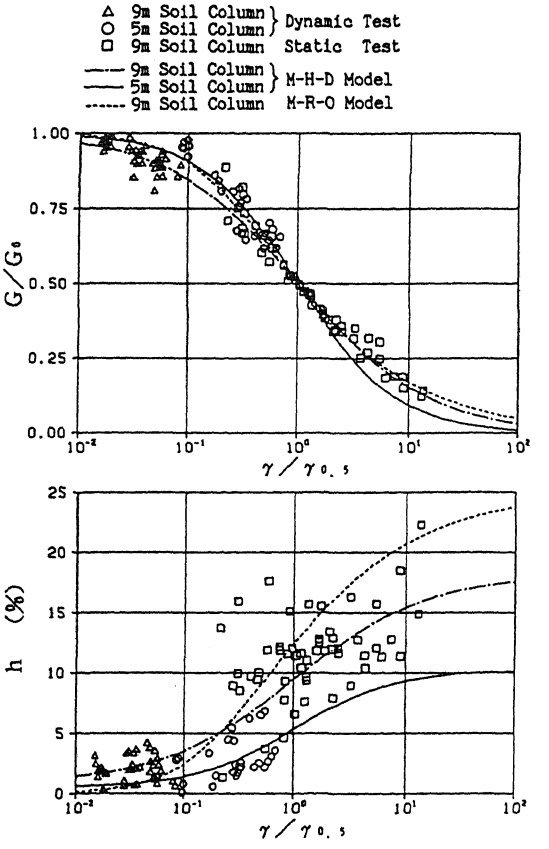

Fig. 10 Strain dependency of shear modulus and damping ratio of soil columns

3.3 Evaluation by inverse analysis

The inverse analyses were conducted using the measured data of the tests in order to clarify the strain dependency of shear modulus and damping ratio of the soil columns quantitatively.

In the dynamic torsional tests, the soil columns were represented by one-stick lumped mass models for torsional mode, as shown in Fig. 9, and complex torsional spring constants in the lumped mass models were calculated using the loading moment and the measured accelerations as input in each loading step. Then, shear moduli and damping ratios of the soil columns at each shear strain were calculated using the formula of the torsional spring constant of a cylinder.

In the static torsional tests, the soil column was represented by a one-stick discrete model for torsional mode, as shown in Fig. 9, and secant torsional spring constants were calculated using the loading moment and the measured maximum shear strains as input in each loading step. Then, equivalent shear moduli and equivalent damping ratios of the soil column at each shear strain were

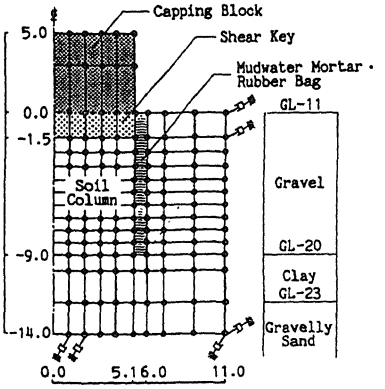

Fig. 11 Model of simulation analysis for dynamic torsional test

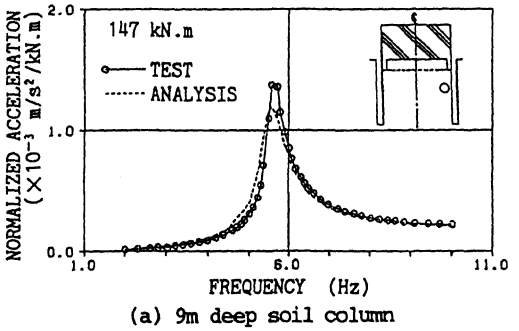

(a) 9m deep soil column

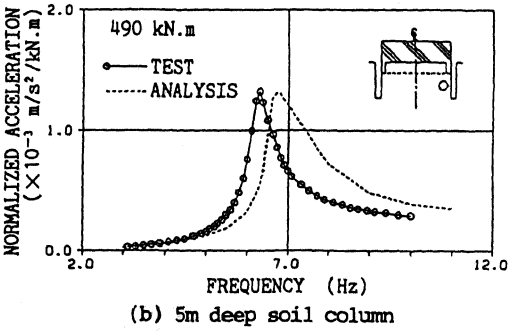

(b) 5m deep soil column

Fig. 12 Comparison of acceleration resonance curves between simulation analysis and test in dynamic torsional test

calculated using hysteresis loops of the calculated shear stress and the measured shear strain.

The shear modulus at small shear strain (G_0), the shear strain at which the shear modulus was reduced to one half, ($\gamma_{0.5}$), and the strain dependency of shear modulus and damping ratio were obtained from the results of the inverse analyses. Fig. 10 shows the strain dependency normalized using G_0 and $\gamma_{0.5}$. As shown in Fig. 10, for the dynamic torsional tests of the 9m deep soil column, the shear modulus ratio (G/G_0) is reduced to about 0.9

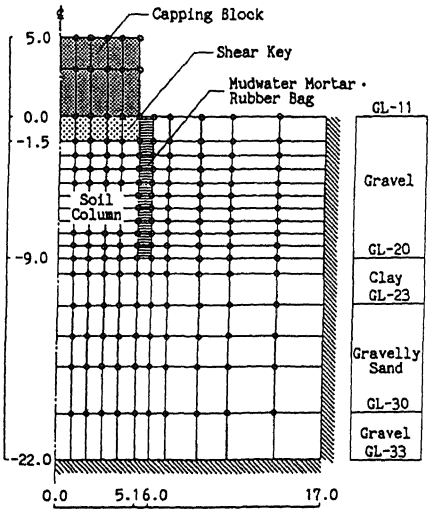

Fig. 13 Model of simulation analysis for static torsional test

and the damping ratio (h) increases approximately from 2% to 3% as the shear strain increases, and for the dynamic torsional tests of the 5m deep soil column, the shear modulus ratio is reduced to about 0.65 and the damping ratio increases approximately from 2% to 5% as the shear strain increases. For the static torsional tests of the 9m deep soil column, the shear modulus ratio is reduced approximately from 0.75 to 0.2 and the damping ratio increases approximately from 8% to 20% as the shear strain increases.

4 SIMULATION ANALYSIS

The objective of the simulation analysis is to validate the applicability of existing analytical methods used hereafter.

4.1 Dynamic torsional tests

From the test results, accumulation of the excess pore water pressure was not observed and the nonlinearity of the response was not strongly indicated. Thus, the equivalent linear method using axi-symmetric grid models was seleced for the simulation analysis. The axi-symmetric grid model consists of nodes having one degree of freedom in circumferential direction and torsional springs which connect adjacent nodes, as shown in Fig. 11. As for soil properties of the soil columns, G_0 and $\gamma_{0.5}$ were given from the results of the inverse analyses, and the strain dependency of shear modulus and damping ratio was given from regression curves using a modified Hardin-Drnevich model (M-H-D model) for each of the 9m and 5m deep soil

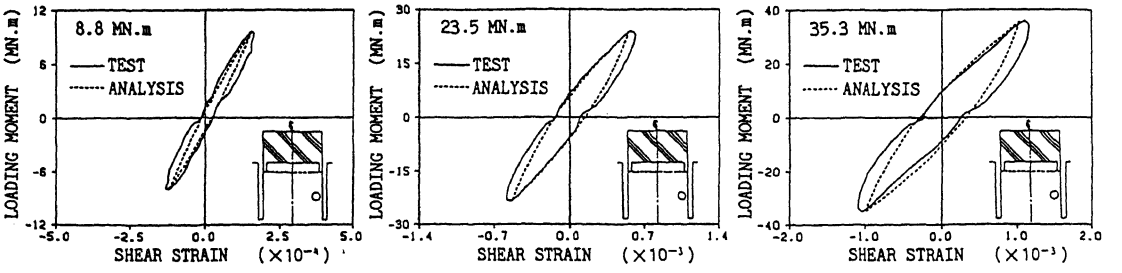

Fig. 14 Comparison of shear srain-loading moment curves at final cycle between simulation analysis and test in static torsional test

columns respectively, as shown in Fig. 10. Material properties of the mudwater mortar and the rubber bags were given from the results of laboratory tests.

Fig. 4 and Fig. 12 show the results of the simulation analyses as compared with the test results. As shown in Fig. 12, the resonance frequency of the 5m deep soil column obtained by the simulation analysis is a little higher than that obtained by the test. Regarding the amplitude of acceleration and shear strain, the calculated results are in good agreement with the measured ones for both the 9m and 5m deep soil columns and the nonlinear responses due to increase of loading moment are well simulated in the small to medium shear strain range.

4.2 Static torsional tests

The nonlinear method with a hysteretic curve model using an axi-symmetric grid model was seleced in order to simulate hysteresis loops on cyclic shear deformation. The axi-symmetric grid model consists of nodes and torsinal springs like the analytical model for the dynamic torsional tests, as shown in Fig. 13. As a hysteretic curve model, a modified Ramberg-Osgood model (M-R-O model) was adopted for torsional springs of the soil. As for soil properties of the soil column, G_0 and $\gamma_{0.5}$ were given from the results of the inverse analyses, and the strain dependency of shear modulus and damping ratio was given from regression curves using a M-R-O model, as shown in Fig. 10. Material properties of the mudwater mortar and the rubber bags were given from the results of laboratory tests.

Fig. 6 and Fig. 14 show the results of the simulation analyses as compared with the test results. In Fig. 14, the comparison at the final cycle is indicated. From these figures, the hysteretic curves as calculated in the simulation analyses are in good agreement with the measured ones and the nonlinear responses due to increase of loading moment are successfully simulated in the large level of shear strain of 10^{-3}.

5 CONCLUSIONS

From the results of the cyclic torsional tests on the large-scale soil columns prepared in-situ and the simulation analyses, the following principal conclusions are obtained.

1. It was confirmed that the gravel layer subjected to shear strains in the small level of 10^{-5} to the large level of 10^{-3} showed decrease in shear modulus and increase in damping ratio due to the strain dependency of gravel material in cyclic loading.
2. The excess pore water pressure did not accumulate in the shear strain range smaller than 10^{-4}.
3. The volumetric deformation due to the dilatancy accumulated in the direction of compression with increasing number of loading in the shear strain range larger than 10^{-3}.
4. It was verified that the equivalent linear method was applicable to response analyses of gravel layer subjected to shear strains in the small to medium range.
5. It was verified that the nonlinear method with a hysteretic curve model could simulate the cyclic shear deformaion of gravel layer subjected to shear strains in the large level.

ACKNOWLEDGEMENTS

This work was carried out by NUPEC as the project sponsored by the Ministry of International Trade and Industry of Japan. This work was reviewed by "Committee of Verification Tests on Siting Technology for High Seismic Structures" of NUPEC. The authors wish to express their gratitude for the cooperation and valuable suggestions given by every committee member.

REFERENCE

Watabe,M. et al. 1991 : Large scale field tests on Quaternary sand and gravel deposits for seismic siting technology, Proc. 2nd International Conference on Recent Advances in Geotechnical Earthquake Engineering and Soil Dynamics, St. Louis, pp.271-289.